Fabrication of Complex Architectures Using Electrodeposition into Patterned Self-Assembled Monolayers

ARTICLE *in* NANO LETTERS · JUNE 2006

Impact Factor: 13.59 · DOI: 10.1021/nl060368f · Source: PubMed

NANO LETTERS

2006
Vol. 6, No. 5
1023−1026

Fabrication of Complex Architectures Using Electrodeposition into Patterned Self-Assembled Monolayers

Noshir S. Pesika,[†] A. Radisic,[‡] Kathleen J. Stebe,*[,†,‡] and Peter C. Searson*[,‡]

Department of Chemical and Biomolecular Engineering and Department of Materials Science and Engineering, Johns Hopkins University, Baltimore, Maryland 21218

Received February 17, 2006

ABSTRACT

Patterned self-assembled monolayers (SAMs) on solid surfaces can be used to direct electrodeposition to occur at specific locations. In previous work, single deposition steps have been used to create islands or lines in patterned SAMs. In this paper we present strategies for creating more complex structures, including via-like structures and multicomponent lines. We also show how finite size effects can be exploited to produce arrays of single-crystal islands.

Patterned self-assembled monolayers (SAMs) provide spatial control over surface properties and enable surface processes to be directed to occur at specific locations. The ability of patterned SAMs to direct electrodeposition offers unique possibilities in the fabrication of a range of materials and structures but has not been widely explored.

There are two general approaches for patterning SAMs. In the first approach, a SAM is formed on a surface and the pattern created using an electron,[1−3] photon,[4,5] or ion beam.[6] Irradiation of thiol SAMs results in degradation of the monolayer forming various fragments, unsaturated bonds, and sulfides.[7,8] Alternatively, irradiation may induce cross-linking, resulting in selective deposition or etching in the regions that were not irradiated, analogous to using a negative resist in conventional lithography.[2,3,9]

Sondag-Huethorst et al.[1] reported on electrochemical deposition of copper lines on docosanethiol ($CH_3(CH_2)_{21}SH$) SAMs patterned using e-beam lithography. Copper deposition occurred in the SAM-free regions at −0.15 to −0.2 V (SCE) although deposition was isotropic, with significant lateral growth. At more negative potentials, deposition occurred in both SAM-free and SAM-modified regions. Kaltenpoth et al.[3] reported copper deposition on ODT ($CH_3(CH_2)_{17}SH$) SAMs modified by e-beam irradiation. At −0.20 and −0.25 V (Ag/AgCl), copper deposition occurred in the SAM-irradiated regions. Felgenhauer et al.[2] showed that irradiation of 1,1′-biphenyl-4-thiol ($C_6H_5-C_6H_4-SH$) and 4′-(methyl-biphenyl-4-yl)dodecylthiol ($CH_3-C_6H_4-C_6H_4-(CH_2)_{12}-SH$) SAMs results in cross-linking of the biphenyl layer and deposition of copper occurred preferentially in the un-irradiated regions.

In the second approach, the patterned SAM can be transferred to the substrate by stamping. Stamping, or soft lithography, has the advantage that it is not a serial technique. Moffat and Yang[10] reported on the electrodeposition of 5 μm × 5 μm nickel islands using soft lithography to stamp a patterned hexadecanethiol ($CH_3(CH_2)_{15}SH$) SAM onto a copper surface. Islands up to 120 nm in thickness were deposited in the surfactant-free regions maintaining the fidelity of the pattern; for higher features lateral growth was observed.

Kumar and Whitesides[11] used stamped SAMs of hexadecanethiol ($CH_3(CH_2)_{15}SH$) as a mask for electroless deposition of nickel on gold. At elevated temperatures, nickel deposited in the SAM-free regions and not in the SAM-modified regions. However, the density of defects was relatively large due to the formation of hydrogen bubbles on the surface and the influence of the elevated temperature on the SAM.

In previous work[12] we have shown that patterned alkanethiol SAMs can be used to direct deposition of gold or silver to SAM-modified or SAM-free regions depending upon the potential and the length of the alkane chain. At small overpotentials, deposition occurs only in the SAM-free regions. At a threshold potential that is dependent on chain length, deposition occurs in the SAM-free regions as well as at defects in the SAM-covered regions. At more negative potentials, deposition occurs in both SAM-free and SAM-modified regions but occurs preferentially in the SAM-modified regions. This is analogous to a positive resist in conventional lithography. Finally, at more negative potentials,

* Corresponding authors. E-mail: searson@jhu.edu, kjs@jhu.edu.
[†] Department of Chemical and Biomolecular Engineering.
[‡] Department of Materials Science and Engineering.

10.1021/nl060368f CCC: $33.50
Published on Web 04/04/2006

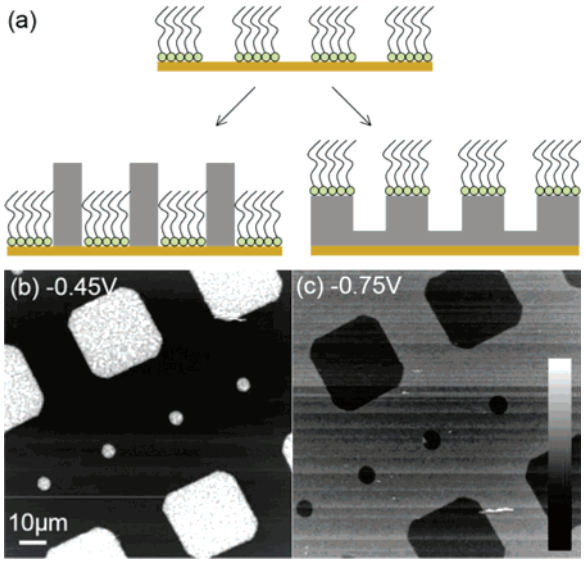

Figure 1. (a) Schematic illustration of electrochemical deposition onto a SAM-modified surface illustrating deposition in the SAM-free regions (positive resist) and preferential deposition in the SAM-modified regions (negative resist). (b) AFM images of silver features deposited onto an ODT-modified gold substrate with an array of 25 μm SAM-free squares and 5 μm SAM-free circles. Silver was deposited at (a) −0.45 V (Ag/AgCl) and (b) −0.75 V (Ag/AgCl). In all cases 0.15 C cm^{-2} silver was deposited. The maximum heights in the images are (a) 800 nm and (b) 500 nm.

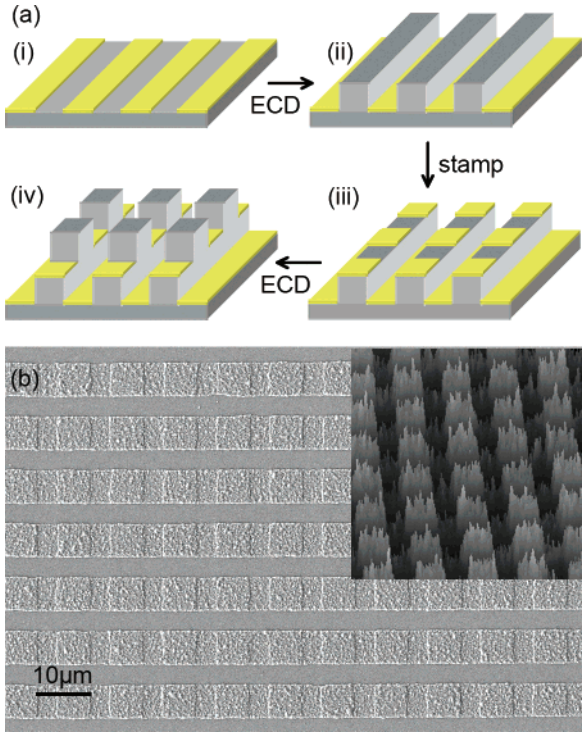

Figure 2. (a) Schematic illustration of the steps for fabrication of via-like structures: (i) SAM-modified lines created by stamping; (ii) electrochemical deposition (ECD) results in the formation of lines; (iii) after a second stamping step SAM-modified squares are formed on the lines; (iv) electrochemical deposition results in the formation of vias on the lines. (b) Plan view SEM image of silver squares formed on silver lines. The inset shows an AFM image of the same structure.

electrochemical desorption of the SAM results in uniform deposition over the whole surface.

These examples illustrate that patterned SAMs can be used to direct electrodeposition and to produce feature sizes up to several hundred nanometers in height without significant lateral growth. While many fundamental issues remain to be addressed, the purpose of this paper is to show that the combination of electrodeposition and stamped SAMs are potentially versatile tools for creating complex, two- and three-dimensional structures. We demonstrate the fabrication of via-like structures, multicomponent lines, and single-crystal island arrays.

Octadecanethiol (ODT, Aldrich, 98.5% purity) SAMs were transferred to thermally evaporated silver or gold substrates using poly(dimethylsiloxane) (PDMS) stamps (Dow Corning, Sylgard 184). Ethanol (Aldrich, 200 proof, ACS grade) was used as the solvent to prepare stock 1−4 mM alkanethiol solutions. In a typical experiment, the PDMS stamp, with the features facing upward, was covered with a solution of alkanethiol in ethanol and allowed to stand for 1 min. The stamp was dried with nitrogen gas and then placed in contact with the substrate for 30 s. The stamp was then removed and the substrate rinsed with ethanol to remove any unbound thiol. The substrate was then dried with nitrogen.

Electrochemical deposition experiments were performed in a three-electrode Teflon cell with a platinum mesh counter electrode and a Ag/AgCl (3 M NaCl) reference electrode (U_{eq} = 0.2 V vs SHE) connected to the cell via a Luggin capillary. All potentials are reported versus the Ag/AgCl reference. Silver was deposited from solution containing 20 mM $KAg(CN)_2$, 0.25 M Na_2CO_3, 0.1 M NaOH, pH ≈ 13. Copper was deposited from solution containing 100 mM $CuSO_4$ and 10 mM H_2SO_4, pH ≈ 2.

Patterned Electrodeposition Using Soft Lithography. Figure 1 shows atomic force microscopy (AFM) images of ODT-patterned gold surfaces after deposition of 0.15 C cm^{-2} silver at −0.45 and −0.75 V. The pattern included 25 μm surfactant-free squares and 5 μm surfactant-free circles. At −0.45 V (Figure 1b) deposition occurs only in the SAM-free regions. There is no evidence of deposition in the SAM-modified regions, illustrating that the SAM acts as an effective barrier to deposition, analogous to a positive resist in conventional lithography. Furthermore, there is no evidence of lateral deposition even though the feature height (about 500 nm) is much greater than the thickness of the SAM (≈2 nm). In contrast, at −0.75 V (Figure 1c) deposition occurs in both SAM-free and SAM-modified regions; however, deposition occurs preferentially in the SAM-modified regions with no evidence of lateral growth. Although the origin of this effect is not known, there are examples of adsorbate-enhanced deposition of silver in the literature. For example, the adsorption of SeCN accelerates the deposition of silver from $KAg(CN)_2$ on planar gold surfaces,[13] and the adsorption of short chain dithiols accelerates the deposition of copper on planar gold surfaces from solution containing $CuSO_4$ and a suppressor such as poly(ethylene glycol).[14] The influence of potential and chain length on deposition has been reported elsewhere.[12]

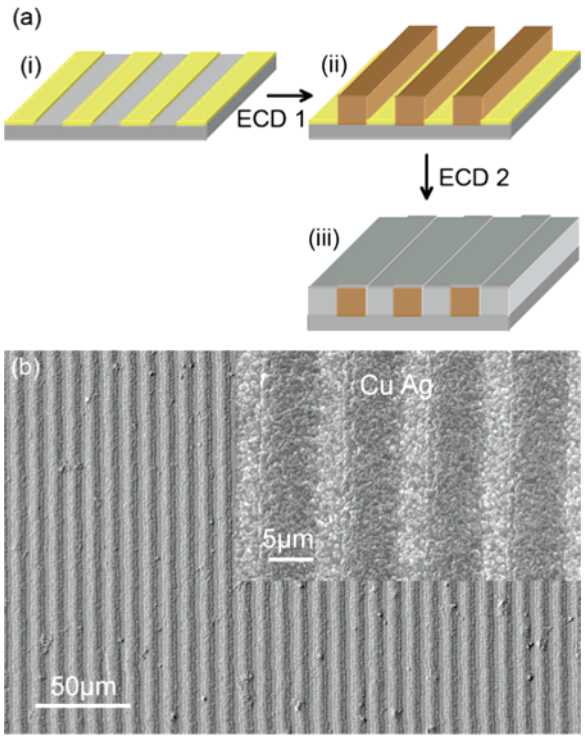

Figure 3. (a) Schematic illustration of the steps for fabrication of multicomponent lines: (i) SAM-modified lines created by stamping; (ii) electrochemical deposition (ECD) of one material in SAM-free regions (low overpotential); (iii) electrochemical deposition of a second material in SAM-modified regions (high overpotential). (b) Plan view SEM image of an array of copper and silver lines formed with one patterning step.

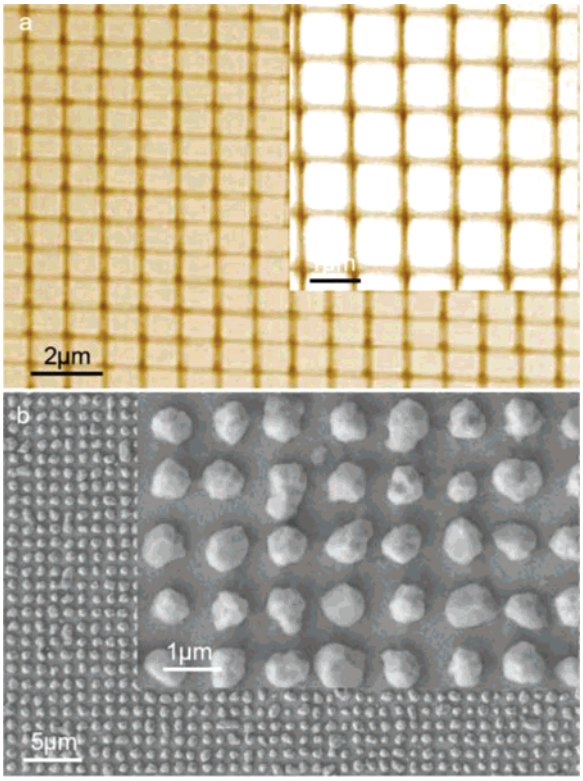

Figure 4. (a) Plan view optical microscope image of the PDMS stamp with a grid pattern of 200 nm wide lines. (b) Plan view SEM image of silver islands deposited on silver with 1 μm × 1 μm SAM-free squares separated by 200 nm SAM-modified lines.

Vias. Figure 2a shows a schematic illustration of the fabrication of via-like structures. In the first step, SAM-modified lines are stamped on the substrate. Electrochemical deposition is then used to deposit a metal into the SAM-free regions. Next, the same stamp is rotated through 90° and used to transfer the SAM to the substrate. The transfer results in SAM-modified squares on the deposited lines since these are the highest features on the substrate. The exposed substrate remains modified by the SAM. In the second deposition step the metal is deposited in the squares along the deposited lines.

Figure 2b shows a plan view SEM image of via-like structure created using the fabrication steps illustrated in Figure 2a. Silver was deposited on an ODT-modified silver surface at −0.47 V (Ag/AgCl) for 8.6 min to form an array of 6 μm wide silver lines on the surface. The substrate was then rotated by 90° and repatterned with octadecanethiol using the same stamp. After a second electrodeposition step at −0.47 V for 5 min, silver islands are deposited only on the SAM-free regions of the previously deposited lines. There is no evidence of deposition in the ODT-modified lines on the substrate during either of the two deposition steps. The heights of the lines and islands determined from AFM images are 169 and 120 nm, respectively, in excellent agreement with the values estimated from the deposition charge (167 and 139 nm). In this technique, a three-dimensional architecture is formed with two stamping steps and two electrodeposition steps. The same structure fabricated by conventional lithographic techniques would require two sequences of coating with photoresist, exposure and developing, deposition, and lift-off.

Multicomponent Lines. A combination of deposition in the SAM-free regions and preferential deposition in the SAM-modified regions can be used to deposit two different materials in the same plane with one lithographic step. A schematic illustration of the approach is shown in Figure 3a. First, SAM-modified lines are patterned on a substrate by stamping. Next a metal is electrodeposited into the SAM-free regions at small overpotentials. Finally, a second metal is deposited at more negative potentials where deposition occurs preferentially in the SAM-modified regions.

Figure 3b shows a plan view SEM image demonstrating the ability to create multicomponent lines by sequentially exploiting positive and negative resist modes. A line pattern was created on a gold substrate and used as a positive resist for copper deposition at −0.16 V (Ag/AgCl) for 2 min resulting in copper lines about 500 nm high. The same substrate was then used in negative resist mode to deposit silver at −0.65 V for 8.5 min between the copper lines. The resulting features were lines of copper between lines of silver. Recall that the negative resist mode is not completely selective and that there is also some silver deposition on the copper lines although it is sufficiently thin that the contrast in the SEM image is dominated by the underlying copper. The composition of the lines was confirmed by energy dispersive spectroscopy. A key feature of this process is that

the creation of this multicomponent structure required only one lithographic step.

Arrays of Single-Crystal Islands. In electrodeposition, the deposition of a metal on a foreign metal substrate often proceeds through island growth. Depending on the size of the patterned features (i.e., SAM-free regions) and their lateral spacing, a variety of finite size effects can influence the growth dynamics. For example, the nucleus density N in electrodeposition is strongly dependent on the deposition potential and the solution chemistry. As long as the area L^2 of a square feature is much larger than the average area per island, i.e., $L^2 \gg 1/N$, then islands can grow and coalesce to fill the feature, as illustrated in Figures 1−3. However, as $L^2 \rightarrow 1/N$, significant differences in the nucleation and growth dynamics are expected.

Figure 4 shows an example illustrating that finite size effects can be exploited in controlling nucleation and island growth. In this case silver was deposited onto an ODT-patterned silver surface with 1 μm × 1 μm SAM-free squares separated by 200 nm SAM-modified lines. Silver was deposited at −0.42 V (Ag/AgCl) for 63 min. The SEM images show that in most cases a single island has nucleated in each SAM-free square producing an array of single-crystal clusters. Thus we can infer that at this potential, the island density $N \leq 10^8$ cm^{-2}. The average island diameter of about 750 nm is in excellent agreement with the value (766 nm) predicted from the deposition charge (0.2 C cm^{-2}) assuming hemispherical islands and a deposition efficiency of 1.0. While many fundamental issues remain to be resolved, such as the influence of the spacing of the SAM-free squares, the deposition potential, and the solution chemistry, this example illustrates that finite size effects can be exploited to produce single-crystal island arrays. Such arrays are of interest for applications such as catalysts for nanowire and nanotube growth.

Acknowledgment. This work was supported by the JHU MRSEC (NSF Grant Number DMR05-20491).

References

(1) Sondag-Huethorst, J. A. M.; Vanhelleputte, H. R. J.; Fokkink, L. G. J. Generation of Electrochemically Deposited Metal Patterns by Means of Electron-Beam (Nano)Lithography of Self-Assembled Monolayer Resists. *Appl. Phys. Lett.* **1994**, *64* (3), 285−287.

(2) Felgenhauer, T.; Yan, C.; Geyer, W.; Rong, H. T.; Golzhauser, A.; Buck, M. Electrode modification by electron-induced patterning of aromatic self-assembled monolayers. *Appl. Phys. Lett.* **2001**, *79* (20), 3323−3325.

(3) Kaltenpoth, G.; Volkel, B.; Nottbohm, C. T.; Golzhauser, A.; Buck, M. Electrode modification by electron-induced patterning of self-assembled monolayers. *J. Vacuum Sci. Technol., B* **2002**, *20* (6), 2734−2738.

(4) Takehara, K.; Yamada, S.; Ide, Y. Use of the Laser-Desorption Technique for the Preparation of a Mixed-Thiol Monolayer on a Gold Electrode. *J. Electroanal. Chem.* **1992**, *333* (1−2), 339−344.

(5) Dulcey, C. S.; Georger, J. H.; Chen, M. S.; McElvany, S. W.; OFerrall, C. E.; Benezra, V. I.; Calvert, J. M. Photochemistry and patterning of self-assembled monolayer films containing aromatic hydrocarbon functional groups. *Langmuir* **1996**, *12* (6), 1638−1650.

(6) Gillen, G.; Wight, S.; Bennett, J.; Tarlov, M. J. Patterning of Self-Assembled Alkanethiol Monolayers on Silver by Microfocus Ion and Electron-Beam Bombardment. *Applied Physics Lett.* **1994**, *65* (5), 534−536.

(7) Heister, K.; Zharnikov, M.; Grunze, M.; Johansson, L. S. O.; Ulman, A. Characterization of X-ray induced damage in alkanethiolate monolayers by high-resolution photoelectron spectroscopy. *Langmuir* **2001**, *17* (1), 8−11.

(8) Muller, H. U.; Zharnikov, M.; Volkel, B.; Schertel, A.; Harder, P.; Grunze, M. Low-energy electron-induced damage in hexadecanethiolate monolayers. *J. Phys. Chem. B* **1998**, *102* (41), 7949−7959.

(9) Geyer, W.; Stadler, V.; Eck, W.; Zharnikov, M.; Golzhauser, A.; Grunze, M. Electron-induced cross-linking of aromatic self-assembled monolayers: Negative resists for nanolithography. *Appl. Phys. Lett.* **1999**, *75* (16), 2401−2403.

(10) Moffat, T. P.; Yang, H. Patterned Metal Electrodeposition Using an Alkanethiolate Mask. *J. Electrochem. Soc.* **1995**, *142* (11), L220−L222.

(11) Kumar, A.; Biebuyck, H. A.; Whitesides, G. M. Patterning Self-Assembled Monolayers—Applications in Materials Science. *Langmuir* **1994**, *10* (5), 1498−1511.

(12) Pesika, N. S.; Fan, F. Q.; Searson, P. C.; Stebe, K. J. Site-selective patterning using surfactant-based resists. *J. Am. Chem. Soc.* **2005**, *127* (34), 11960−11962.

(13) Baker, B. C.; Freeman, M.; Melnick, B.; Wheeler, D.; Josell, D.; Moffat, T. P. Superconformal electrodeposition of silver from a KAg(CN2)−KCN−KSeCN electrolyte. *J. Electrochem. Soc.* **2003**, *150* (2), C61−C66.

(14) Moffat, T. P.; Wheeler, D.; Josell, D. Electrodeposition of copper in the SPS−PEG−Cl additive system. I. Kinetic measurements: Influence of SPS. *J. Electrochem. Soc.* **2004**, *151* (4), C262−C271.

NL060368F